frontiers | Frontiers in Environmental Chemistry

TYPE Original Research
PUBLISHED 13 March 2024
DOI 10.3389/fenvc.2024.1373320

OPEN ACCESS

EDITED BY
Erick R. Bandala,
DASCO Inc., United States

REVIEWED BY
Eduardo Francisco Pino Lopez,
University of Santiago, Chile
Monica Cerro-Lopez,
University of the Americas Puebla, Mexico

*CORRESPONDENCE
Jan M. Macak,
jan.macak@upce.cz
Beata J. Stanisz,
bstanisz@ump.edu.pl

†These authors have contributed equally to this work

RECEIVED 19 January 2024
ACCEPTED 27 February 2024
PUBLISHED 13 March 2024

CITATION
Sepúlveda M, Musiał J, Saldan I, Chennam PK, Rodriguez-Pereira J, Sopha H, Stanisz BJ and Macak JM (2024), Photocatalytic degradation of naproxen using TiO_2 single nanotubes. *Front. Environ. Chem.* 5:1373320. doi: 10.3389/fenvc.2024.1373320

Photocatalytic degradation of naproxen using TiO_2 single nanotubes

Marcela Sepúlveda[1†], Joanna Musiał[2†], Ivan Saldan[3], Pavan Kumar Chennam[3], Jhonatan Rodriguez-Pereira[1,3], Hanna Sopha[1,3], Beata J. Stanisz[2*] and Jan M. Macak[1,3*]

[1]Center of Materials and Nanotechnologies, Faculty of Chemical Technology, University of Pardubice, Pardubice, Czechia, [2]Chair and Department of Pharmaceutical Chemistry, Poznan University of Medical Sciences, Poznań, Poland, [3]Central European Institute of Technology, Brno University of Technology, Brno, Czechia

Herein, TiO_2 single-tube (TiO_2 ST-NT) powders with and without magnetite Fe_3O_4 nanoparticles (TiO_2 ST-NT@Fe_3O_4NPs) are presented for the first time as excellent photocatalysts for the degradation of one of the most popular non-steroidal anti-inflammatory drugs (NSAIDs), naproxen (NPX). The TiO_2 ST-NT powders were synthesized by anodization followed by etching of the double wall, bending, sonication, ultra-centrifugation, and finally annealing at 600°C. A part of the obtained TiO_2 ST-NT powders was decorated with Fe_3O_4 nanoparticles using a simple one-step decoration process. The best photocatalytic performance of TiO_2 ST-NT and TiO_2 ST-NT@Fe_3O_4NPs powders was obtained under the white light (6.2×10^{-4} s^{-1}) and the blue light (2.7×10^{-4} s^{-1}), respectively. During NPX photodegradation using TiO_2 ST-NT powders, three main NPX transformation products (P1, P2, and P3) were detected. Upon excitation with the blue light illumination, TiO_2 ST-NT@Fe_3O_4NPs powders exhibited higher performance (~80%) than TiO_2 ST-NT powders (~23%) within 1 h, resulting in an approximately three times increased photocatalytic rate constant. Moreover, under simulated sunlight conditions, TiO_2 ST-NT powders demonstrated remarkable activity, achieving a 94% NPX degradation within 1 h. TiO_2 ST-NT and TiO_2 ST-NT@Fe_3O_4NPs powders represent excellent photocatalysts for NPX degradation.

KEYWORDS

TiO_2 single nanotube, Fe_3O_4 nanoparticles, photocatalysis, naproxen, water treatment

Abbreviations: AOPs, advanced oxidation processes; EDX, energy dispersive X-ray Analysis; HPLC-DAD, high-performance liquid chromatography with photodiode-array detection; HRTEM, high-resolution scanning transmission electron microscopy; NSAIDs, non-steroidal anti-inflammatory drugs; NPs, nanoparticles; NPX, naproxen; P1, P2, and P3, transformation products; SEM, scanning electron microscopy; STEM, scanning transmission electron microscopy; TiO_2 NT, TiO_2 nanotube; TiO_2 ST-NT, TiO_2 single-tube nanotube powders; TiO_2ST-NT@Fe_3O_4NPs, TiO_2 single-tube nanotube powders decorated with Fe_3O_4 nanoparticles; XPS, X-ray photoelectron spectroscopy; XRD, X-ray powder diffraction.

1 Introduction

In recent years, efforts have been carried out to improve the elimination of pharmaceutical compounds found in various water sources worldwide, including water inlets and outlets, streams, rivers, and groundwater. Pharmaceutical pollutants, persistent in aquatic environments, can have harmful effects on the human health, including kidney problems, skin diseases, and poisoning (Margot et al., 2015; Petrie et al., 2015). Non-steroidal anti-inflammatory drugs (NSAIDs) have gained particular attention as an often-detected class of pollutants because of their stability and resistance. NSAIDs discharge to the environment can originate from hospitals, pharmaceutical industry effluents, and domestic wastewater, which results from their frequent use, over-the-counter accessibility, and high excretion rates (Memmert et al., 2013; Simon and Evan Prince, 2017).

Many solutions have been proposed to reduce or eliminate organic pollutants in wastewater and improve its quality. Advanced oxidation processes (AOPs) have emerged as a viable option for treating a wide range of emerging contaminants, including pharmaceuticals (Stasinakis, 2008; Miklos et al., 2018; Anjali and Shanthakumar, 2019). The efficacy of AOPs is determined by the generation of reactive oxygen species, primarily hydroxyl radicals (OH•). Due to their non-selective nature, OH• can degrade various organic compounds present in water and wastewater, forming carbon dioxide, water, and mineral acids (Legrini et al., 1993). The most used AOPs include ozone-based processes (Abromaitis et al., 2022), Fenton reaction (Im et al., 2015a), advanced oxidation with persulfate (Ge et al., 2021), and photocatalysis (Ye et al., 2018). Among these, the photocatalytic process using a semiconductor material has been extensively researched for the elimination, degradation, and mineralization of organic compounds in aqueous systems (Li and Li, 2001; Choi et al., 2007).

One of the most widely investigated semiconductors is TiO_2, a very efficient photocatalyst used for the degradation of pharmaceutical contaminants in water (Mills et al., 1993; Mills and Le Hunte, 1997; Hashimoto et al., 2005; Ni et al., 2007). The crystallinity of TiO_2 plays a crucial role in photocatalysis (Tanaka et al., 1991; Li et al., 2012). For instance, the anatase phase exhibits superior activity when exposed to UV illumination, while the presence of mixed anatase-rutile crystalline phases has been associated with photoactivity at longer wavelengths in the visible light region (Collins-Martinez et al., 2007; Solís-Casados et al., 2017).

The application of TiO_2 in the photocatalytic oxidative remediation of pharmaceutically polluted water has already been reported (Molinari et al., 2006; Coleman et al., 2007). Different shapes of TiO_2 such as nanoparticles (Kanakaraju et al., 2015), nanofibers (Doh et al., 2008), and nanotubes (Albu et al., 2007; Macak et al., 2007; García-Valverde et al., 2014) can be used as a photocatalyst. The most popular ways to synthesize TiO_2-based nanomaterial include sol-gel (Akpan and Hameed, 2010), solsolvothermal (Zhou et al., 2010), hydrothermal (García-Valverde et al., 2014; Kasuga et al., 1999), and anodization (Macak et al., 2008). TiO_2 nanotube (TiO_2 NT) layers obtained via anodization have been particularly useful for the degradation of pharmaceuticals (Im et al., 2015a; Qian et al., 2021).

Among the NSAIDs, naproxen (NPX), which is widely prescribed for skeleton-muscle pain or inflammatory rheumatic disorders, is one of the most frequently detected pharmaceutical residues in water bodies (Todd and Clissold, 1990; Stovitz and Johnson, 2003). TiO_2 nanoparticles and TiO_2 nanotube (TiO_2 NT) layers have been reported in the elimination of NPX from various wastewater matrices (Im et al., 2015a; Kanakaraju et al., 2015). Different shapes of TiO_2 unmodified (Méndez-Arriaga et al., 2008b, 2008a; Jallouli et al., 2016a; Kanakaraju et al., 2016a) and modified for instance with Ce (Hao et al., 2023), MoS_2 (Sheydaei et al., 2022), and Cu-S (Amini et al., 2020) in the removal of different drugs show a positive impact on the degradation rates as shown in Supplementary Tables S1, S2. However, only one publication focused on TiO_2 NT layers as a catalyst using AOPs to determine their effectiveness in degrading NPX under ultrasonic radiation. In that study was demonstrated a remarkable 96.0% improvement in NPX degradation efficiency when TiO_2 NT layers were present, as opposed to their absence (Im et al., 2015).

To further enhance the photocatalytic performance of TiO_2-based nanomaterials and also to extend the light absorption in the visible spectral region, Fe_3O_4 nanoparticles (NPs) were incorporated into TiO_2-based nanomaterials (Liu et al., 2016; Bi et al., 2019; Yilmaz et al., 2020). Apart from the more favorable light absorption, this enhancement can be attributed to the efficient separation of h^+ and e^-, which occurs by reducing iron ions into Fe^{2+} or Fe^0 (Li et al., 2017). Additionally, whenever a magnetic field can be applied to the material or system used, this modification facilitates and accelerates the separation of the liquid phase from the solid photocatalyst, using an external magnet, without the need for centrifugation or filtration. Recently, it was shown that TiO_2 single-tube (TiO_2 ST-NT) powders, derived from TiO_2 NT layers, present an excellent photocatalytic performance under UV light using methylene blue as a model dye (Beketova et al., 2020). The TiO_2 ST-NT powders were synthesized by anodization, followed by an etching process, and modification with Fe_3O_4 (magnetite) NPs, resulting in TiO_2 nanotube powders modified with Fe_3O_4 NPs (TiO_2 ST-NT@Fe_3O_4NPs) as a guidable photocatalyst (Beketova et al., 2020). The effect of the annealing temperature of TiO_2 ST-NT and TiO_2 ST-NT@Fe_3O_4NPs powders on the photocatalytic performance was evaluated, revealing that the best results were obtained after annealing at 600°C (Sepúlveda et al., 2023).

To the best of our knowledge, this study is the first to report on the photocatalytic performance of TiO_2 ST-NT and TiO_2 ST-NT@Fe_3O_4NPs powders for the degradation of NPX under visible light of different wavelengths. The aim of this study was to i) obtain hybrid photocatalytic materials based on TiO_2 ST-NT powders and Fe_3O_4 NPs, and ii) assess their photocatalytic activity. The TiO_2 ST-NT and TiO_2 ST-NT@Fe_3O_4NPs powders annealed at 600°C were tested for the photocatalytic degradation of NPX using visible light: the blue light (λ_{max} = 425 nm), the green light (λ_{max} = 525 nm), and the white light. The kinetics of degradation and the possible NPX degradation products were also discussed.

2 Materials and methods

2.1 Synthesis of TiO_2 ST-NT powders

To obtain TiO_2 single-tube (TiO_2 ST-NT) powders, the following procedure was employed, as described in our previous work (Sepúlveda et al., 2023). In brief, TiO_2 nanotube (TiO_2 NT) layers were synthesized on Ti foils (127 μm thick, Sigma-Aldrich) in ethylene glycol (Anhydrous, 99.8% CAS-No: 107-21-1, Sigma-Aldrich) -based electrolyte containing 10% water and 0.15 M NH4F (ACS reagent, purity ≥98.0%, CAS-No: 12125-01-8, Sigma-Aldrich) at 100 V for 4 h using a high-voltage potentiostat (PGU-200 V, IPS Elektroniklabor GmbH) (Das et al., 2017). Afterward, the TiO_2 NT layers were etched to remove the inner wall of the tubes (Motola et al., 2018). This was achieved by treating the TiO_2 NT layers with piranha solution (H_2SO_4 (Sulfuric acid 96% A.G., CAS-No: 7664-93-9, Penta): H_2O_2 (Hydrogen peroxide 30% A.G., CAS-No: 7722-84-1, Penta) = 3:1) for 16 min at 70°C. Afterwards, the foils were bent to facilitate the removal of TiO_2 NT layers from Ti foils (Beketova et al., 2020).

To transform the TiO_2 NT layers into TiO_2 ST-NT powders, the TiO_2 NT layers were sonicated in isopropanol (98.8% A.G., CAS-No: 67-63-0, Penta) using an ultrasonic bath (FB11203, Fisherbrand) for 5 h at 37 kHz and 100% power. Subsequently, ultra-centrifugation (Optima MAX-XP, Beckman Coulter) at 25,000 g force for 10 min at 25°C was performed to separate the TiO_2 ST-NT powders from the isopropanol. The obtained powders were then annealed at 600°C in a muffle oven with a sweep rate of 2.1°C min^{-1} (Sepúlveda et al., 2023).

Fe_3O_4 (magnetite) NPs were prepared using an oleic acid process approach, as described in our previous works (Beketova et al., 2020; Sepúlveda et al., 2023). As a final step, the TiO_2 ST-NT powders were decorated with Fe_3O_4 NPs using a simple one-step decoration process, resulting in TiO_2 ST-NT@Fe_3O_4NPs powders (Sepúlveda et al., 2023).

2.2 Material characterization

The morphological characterization was performed using a Transmission Electron Microscope Titan Themis 60–300 (Thermo Fisher Scientific) operated at 300 kV equipped with a high-angle annular dark field detector for scanning transmission electron microscopy (HAADF-STEM) and Super-X detector for STEM energy dispersive X-ray (EDX) spectroscopy. The chemical surface composition of TiO_2 ST-NT and TiO_2 ST-NT@Fe_3O_4NPs powders was analysed through X-ray photoelectron spectroscopy (XPS) using an ESCA2SR instrument from Scienta-Omicron. The measurements were conducted with a monochromatic Al Kα X-ray source operating at 250 W. To ensure accuracy, a binding energy scale correction was applied using the C 1s adventitious carbon peak at 284.8 eV. The data analysis was carried out using the CasaXPS program, developed by Casa Software Ltd.

2.3 Photocatalytic performance

To select the suitable light sources, an absorption spectrum NPX, published in the literature was considered (Arany et al., 2013; Jallouli et al., 2016; Yu et al., 2019). Naproxen photocatalytic degradation tests under the illumination of the blue light (λ_{max} = 425 nm, power = 10 W, irradiance = 20 mW/cm^2) or the green light (λ_{max} = 525 nm, power = 10 W, irradiance = 5 mW/cm^2) were carried out in a reactor consisting of three glass vials placed either on magnetic stirrers (when TiO_2 ST-NT powders were used) or on an orbital shaker (when TiO_2 ST-NT@Fe_3O_4NPs powders were used) (Krakowiak et al., 2022; Musial et al., 2022). The tests under the illumination of the white light were conducted in a PhotoCube™ reactor (ThalesNano Inc., Hungary) equipped with four glass vials and four LED panels (32 W each).

During all the experiments, each vial contained 10 mg of the photocatalytic material and 10 mL of 20 mg/L naproxen water solution. The working solution was diluted from a stock solution prepared beforehand by dissolving 100.0 mg of naproxen (PHR 1040, CAS-No: 22204-53-1, Sigma-Aldrich) in 10.0 mL of acetonitrile (HPLC-grade, CAS-No: 75-05-8, Sigma-Aldrich). After adding the photocatalytic material, the mixture was sonicated for 5 min and stirred for 30 min in the dark to reach the adsorption-desorption equilibrium. Then, the light source (blue, green, or white) was turned on. The mixtures were illuminated for 3 h and constantly stirred. Samples of 0.75 mL were taken at the following time points: 0, 15, 30, 60, 120, and 180 min. Collected samples were centrifuged at 10,000 rpm for 20 min. Prior to the HPLC analyses, the samples were additionally filtered through 0.2 μm PTFE syringe filters.

NPX concentrations were measured using an HPLC instrument equipped with a diode array detector (DAD) (Agilent 1,220 Infinity LC System, PerkinElmer, United States), operating at a wavelength of 231 nm, and a Phenomenex Kinetex C18 column (100 × 4.6 mm, 2.6 μm). The flow rate was 1.0 mL/min, and the injected sample volume was 10 μL. The mobile phase consisted of acetonitrile and 1% acetic acid (HPLC-grade, 99.5%–99.9%, CAS-No: 64-19-7, POCH Avantor Poland), 50:50 (v/v).

3 Results and discussion

The X-ray diffraction (XRD) patterns, extensive scanning electron microscopy (SEM) evidence, specific surface areas, high-resolution scanning transmission electron microscopy (HRTEM-STEM-EDX) elemental maps exhibiting the distribution of Ti, Fe, and O, and pore size distributions of TiO_2 ST-NT and TiO_2 ST-NT@Fe_3O_4NPs powders annealed at 600°C have been reported in our previous work (Sepúlveda et al., 2023). To provide a new insight into the materials used, Figure 1 shows TEM images of TiO_2 ST-NT and TiO_2 ST-NT@Fe_3O_4NPs powders, both annealed at 600°C. As shown in Figure 1B, the surface of TiO_2 ST-NT@Fe_3O_4NPs powders exhibits an uniform distribution of Fe_3O_4 NPs on the surface of TiO_2 ST-NT powders.

The surface elemental composition of the TiO_2 ST-NT and TiO_2 ST-NT@Fe_3O_4NPs powders before the photocatalytic measurements was obtained by XPS analysis and it is shown in Supplementary Table S3. The TiO_2 ST-NT@Fe_3O_4NPs powders show a significantly increased amount of C compared to the TiO_2 ST-NT powders due to the Fe_3O_4 NPs modification using an oleic acid process approach. The high-resolution Ti 2p, O 1s, and C 1s XPS spectra of TiO_2 ST-NT powders are shown in

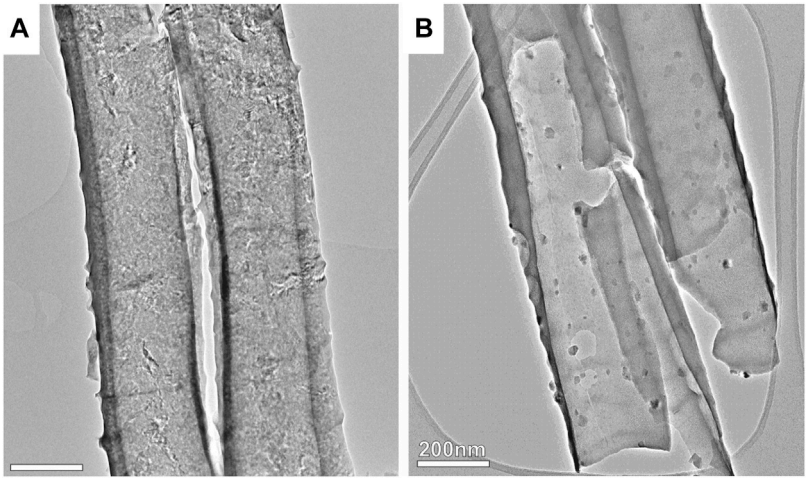

FIGURE 1
Illustrative TEM images of the **(A)** TiO_2 ST-NT and **(B)** TiO_2 ST-NT@Fe_3O_4NPs powders. The scale bar corresponds to the distance of 200 nm.

Supplementary Figure S1. The Ti 2p spectrum exhibits its spin-orbit splitting doublet Ti $2p_{3/2}$ and Ti $2p_{1/2}$ fitted using six components that correspond to three different chemical species. The first doublet (red line) was assigned to Ti^{4+} from the TiO_2 (peaks centered at ~458.7 and 464.4 eV) (Hoyos et al., 2017; Sopha et al., 2020). The second doublet (blue line) is related to Ti^{3+} in the TiO_2 lattice (peaks located at 457.5 and 463.2 eV) (Hoyos et al., 2017; Sopha et al., 2023). The third doublet (olive line) corresponds to non-stoichiometric TiO_x (peaks at 459.9 and 465.6 eV) (Sopha et al., 2020). The O 1s spectrum reveals the presence of four chemical states. The red peak was assigned to O^{2-} or TiO_2 at ~529.9 eV (Hoyos et al., 2017; Sopha et al., 2020). The blue peak is related to –OH at ~530.9 eV (Wu et al., 2017; Sopha et al., 2020), the olive peak corresponds to C-O species at 532.0 eV (Rouxhet and Genet, 2011) and the orange peak evidences the presence of (C=O)-OH at ~533.1 eV (Rouxhet and Genet, 2011). The fitting of the C 1s spectrum was carried out with three different chemical states, adventitious carbon at ~284.8 eV, C-O species at ~286.4 eV and (C=O)-OH at ~288.8 eV (Rouxhet and Genet, 2011).

Supplementary Figure S2 displays the Ti 2p, Fe 2p, O 1s, and C 1s XPS spectra of the TiO_2 ST-NT@Fe_3O_4NPs powders before the photocatalytic measurements. The fitting of the Ti 2p spectrum revealed one doublet suggesting the presence of one titanium oxidation state, Ti^{4+} (peaks located at ~458.6 and ~464.3 eV). In the case of the Fe 2p spectra its corresponding spin-orbit splitting Fe $2p_{3/2}$ and Fe $2p_{1/2}$ is evidenced. The peak fitting suggests the presence of two different oxidation states, in line with the expected states of the Fe_3O_4 NPs. The oxidation states for iron were Fe^{2+} (peaks at ~710.3 and ~723.9 eV), and Fe^{3+} (peaks at ~712.3 and ~725.9 eV) (Tang et al., 2018; Ai et al., 2019). O 1s and C 1s spectra reveal the same chemical species as the TiO_2 ST-NT powders, with the difference in the intensity and a small shifting in the binding energy ~0.4 eV of –OH, C-O and (C=O)-OH species in the O 1s signal.

The photocatalytic performance of the powders was assessed in a series of NPX degradation tests, carried out using light sources of different main wavelengths. Experiments were conducted using either LED lamps emitting either blue (λ_{max} = 425 nm) or green (λ_{max} = 525 nm) light or using a solar simulator emitting white light. NPX degradation was observed in each experiment. Moreover, three main NPX transformation products were detected and monitored throughout the experiments: P1, P2, and P3 (marked according to their detection order, Supplementary Figure S3).

Figure 2A shows the photocatalytic performance of TiO_2 ST-NT powders activated using the blue light illumination. A 60% reduction of NPX initial concentration was noted within 3 h. At the same time, the concentration of all three transformation products, P1, P2, and P3, increased gradually. In the case of TiO_2 ST-NT@Fe_3O_4NPs powders, 92% of NPX was degraded within 3 h (Figure 2B). As for the NPX transformation products, only P1 and P3 appeared – P2 was not formed. At the end of the experiment, the levels of both P1 and P3 were higher than when unmodified ST-NT powder was used. Therefore, modification with Fe_3O_4 NPs enhanced the photocatalytic activity of the TiO_2 ST-NT powders under the blue light illumination.

Upon excitation of the powders with the green light illumination, only 20% NPX degradation was noted in both experiments – when either TiO_2 ST-NT or TiO_2 ST-NT@ Fe_3O_4NPs powders were used. In both tests, the NPX transformation products were detected at a very low level (~1%). Figure 3A shows that all three transformation products appeared when TiO_2 ST-NT powders were used, whereas when TiO_2 ST-NT@ Fe_3O_4NPs powders were used, P2 was not detected (Figure 3B). Noteworthy, P2 was not found during both experiments using Fe_3O_4-modified materials, even if these photocatalysts were more active than bare TiO_2 ST-NTs. There are two possible explanations for this result. First, P2 could be adsorbed on the surface of TiO_2 ST-NT@Fe_3O_4NPs and removed via filtration prior to the HPLC analysis. Adsorption of various pharmaceuticals on iron oxides has already been described (Olusegun et al., 2023). Therefore, it is likely that in the present work, such a phenomenon exists between iron oxides and transformation products of pharmaceuticals, too. Alternatively, when Fe_3O_4-decorated powders were used, P2 could be degraded via photo-Fenton reactions typical for iron oxide-based materials, and thus it was not detected during the analysis (Punjabi et al.,

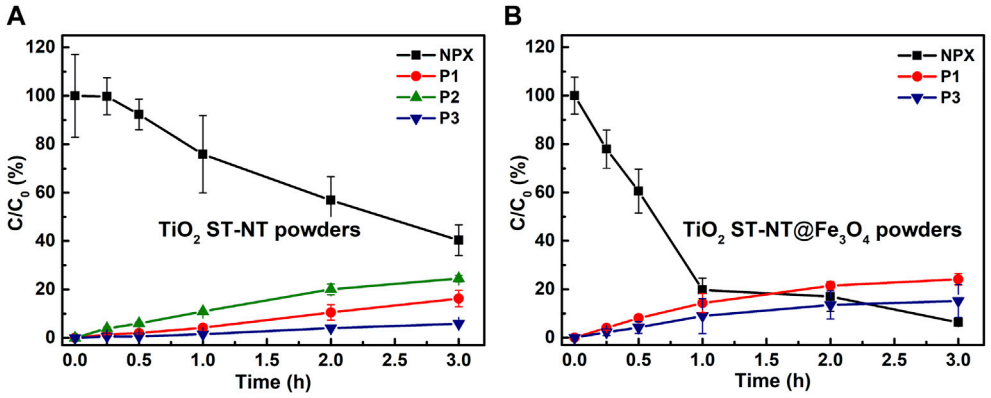

FIGURE 2
Changes in the concentration of NPX and its transformation products (P1, P2, and P3) during the blue light illumination (wavelength ≈425 nm) of the water suspension containing; **(A)** TiO_2 ST-NT powders and **(B)** TiO_2 ST-NT@Fe_3O_4NPs powders as a photocatalyst.

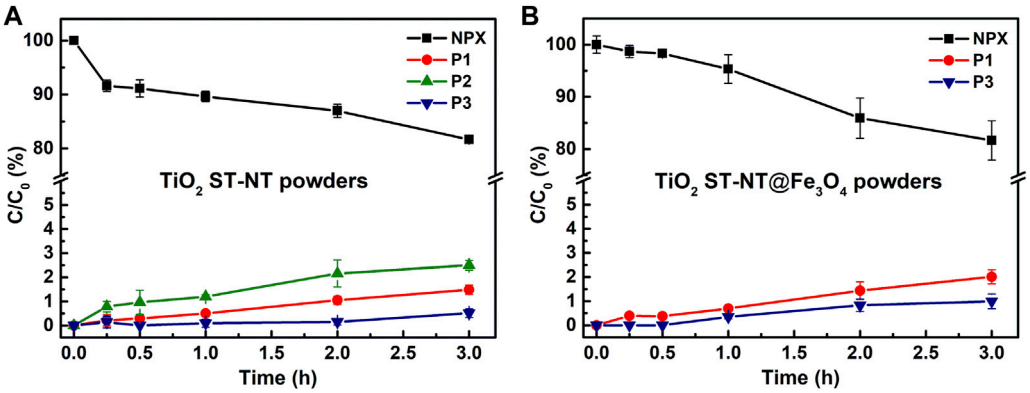

FIGURE 3
Changes in the concentration of NPX and its transformation products (P1, P2, and P3) during the green light illumination (wavelength ≈525 nm) of the water suspension containing; **(A)** TiO_2 ST-NT and **(B)** TiO_2 ST-NT@Fe_3O_4NPs powders.

2018; Olusegun et al., 2023). Two photodegradation mechanisms should be considered for iron oxides – regular excitation of the semiconducting materials and photo-dissolution of iron oxides – and P2 could be more susceptible to the latter, which led to its quick elimination from the system. It is also worth noting that the blue and green LED lamps had the same power. Consequently, the irradiance values differed because they depended on the irradiation wavelength. Although most studies on photocatalytic degradation provide little information on the light source used and this detail is rarely pointed out, it should be considered that differences in irradiance values can affect the photocatalytic degradation rates (Eskandarian et al., 2016; Zaveri et al., 2018).

Among several works on the photocatalytic degradation of pharmaceutical contaminants using TiO_2 combined with Fe-oxides (Amini et al., 2020; Pena-Velasco et al., 2021; Krakowiak et al., 2022) only a few reports show efficient removal rates under the visible light illumination (Sheydaei et al., 2022; Hao et al., 2023). High efficiency is often achieved when other processes, such as ozonation or photoelectrocatalysis, are additionally applied (Amini et al., 2020; Sheydaei et al., 2022). In the present study, we determined the influence of the visible irradiation of a given main wavelength, emitted from a low-power lamp on the TiO_2 ST-NT@Fe_3O_4NPs and noted comparable results. This indicates that the composites display high activity upon excitation with the visible light illumination. Recent studies on photocatalytic removal of commonly used medicines using TiO_2-iron oxide materials and visible light are listed in Supplementary Table S1.

Furthermore, the activity of TiO_2 ST-NT powders upon simulated sunlight excitation was assessed. In this case, PhotoCube™ was used – a reactor equipped with four LED panels emitting white light. 90% of NPX was degraded within 1 h, and a complete removal occurred within 2 h. Figure 4 shows that all three transformation products were detected during the photocatalytic experiment. Noteworthy, at the end of the experiment, not only NPX but also P2 were completely degraded.

NPX degradation under the white light (i.e., using simulated sunlight) occurred faster than under the other light sources, as compared in Table 1 (photocatalytic rate constants) and plotted in Supplementary Figure S3 (degradation curves). It is important to bear in mind that the tests conducted under the blue light and

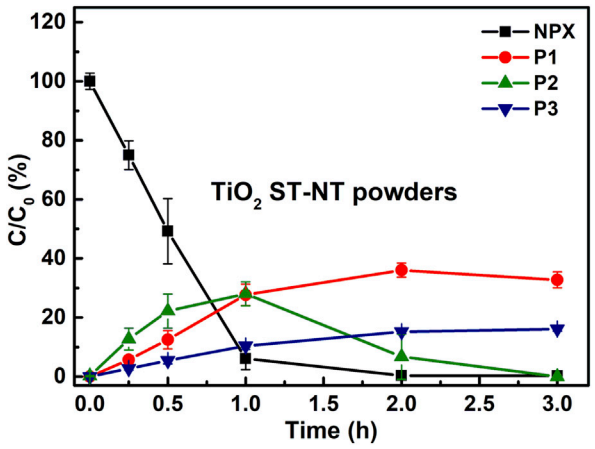

FIGURE 4
Changes in the concentration of NPX and its transformation products (P1, P2, and P3) during the white light illumination of the water suspension containing TiO_2 ST-NT powders.

the white light (Figures 2–4) cannot be directly compared due to the different experimental setups and power of the illumination sources (Musial et al., 2023). Nevertheless, these results confirmed the high activity of unmodified TiO_2 ST-NT powder upon the white light illumination, comparable or higher to NPX degradation efficiencies shown in other photocatalytic studies, listed in Supplementary Table S2 (Uheida et al., 2019; Eslami et al., 2020; Kowalkińska et al., 2023). For instance, Eslami et al. achieved complete NPX removal within 2 h, using polycarbonate coated with N- and S-doped TiO_2, but employed a high-power (350 W) Xe lamp (Eslami et al., 2020). Similar results under comparable conditions (Xe lamp of 125 W) – complete degradation within 1.5 h – were reported by Uheida et al. (2019), using TiO_2 nanoparticles immobilized on polyacrylonitrile/multiwall carbon nanotubes composite nanofiber. However, in this study, only irradiation of a wavelength higher than 420 nm was used, whereas in the present work simulated sunlight conditions also include the participation of the UV-range irradiation in the solar light spectrum. Experiments using TiO_2 ST-NT@Fe_3O_4NPs powders and white light were not conducted due to technical obstacles, because the built-in magnetic stirring precluded using TiO_2 ST-NT@Fe_3O_4NPs powders without an unwanted influence on the degradation rates.

Previous studies have demonstrated that the two main NPX degradation routes are decarboxylation and hydroxylation (demethylation) as one can see in Figure 5 (Kanakaraju et al., 2016; Changanaqui et al., 2020; Jung et al., 2020). Noteworthy, these two routes can occur simultaneously or successively (Méndez-Arriaga et al., 2008b; Fan et al., 2019; Kowalkińska et al., 2023). Another route, dimerization, that leads to the formation of more complex compounds, was also described (Kowalkińska et al., 2023). Interestingly, the dimer formation was reported to depend on the facets exposition of the fluorinated TiO_2. The results of our analyses match previous reports and considerations. During high-performance liquid chromatography with photodiode-array detection (HPLC-DAD) analyses, it was noted that P1 was eluted earlier than NPX and both P2 and P3 later than NPX. This suggests that P1, is a more polar compound than NPX and is a product of NPX hydroxylation, whereas P2 and P3 are products of its decarboxylation. Furthermore, during the NPX degradation experiment using TiO_2 ST-NT powders and simulated sunlight, P2 was completely removed at the end of the experiment. This proves that not only the main tested contaminant but also its transformation products are susceptible to photocatalytic degradation using TiO_2 nanotube layers (Jallouli et al., 2016a).

Prolonged irradiation of the photocatalytic mixture may lead to the complete elimination of the drug transformation products. This is an important observation, as recent research on the toxicity of pharmaceutical pollutants focuses not only on the parent compound but also on the transformation products (Maculewicz et al., 2022). *In vitro* assays using bioluminescent bacteria (*Allivibrio fischeri*), showed that the transformation products displayed higher potential toxicity than the parent compound, but the toxicity of the whole post-degradation mixture was not considered as a major concern (Cazzaniga et al., 2020). In addition, phototransformation products of lower molecular weight were found to be more active towards *A. fisheri*. However, not all the NPX transformation products displayed higher toxicity than the parent compound, which was a proof of the stereostructure-activity relationship (DellaGreca et al., 2003). Other bioassays performed on algae, rotifers, and microcrustaceans proved that phototransformation products displayed higher acute and chronic toxicity than NPX. However, no genotoxic or mutagenic effects were found (Isidori et al., 2005). Moreover, mixtures of NPX and its transformation products proved to be more toxic toward southern toads (*Anaxyrus terrestris*) than NPX alone (Cory et al., 2019). In this regard the complete degradation of pharmaceuticals along with their transformation products during water treatment is necessary. Toxicity assessment of the wastewater effluents should be considered in the design of AOPs-based water remediation systems. All in all, as highly effective photocatalytic materials, TiO_2 ST-NTs powders hold great

TABLE 1 NPX degradation reaction rate constants k (s^{-1}) under the blue light or the white light illumination using TiO_2 ST-NT and TiO_2 ST-NT@Fe_3O_4NPs powders as photocatalysts. r is the correlation coefficient.

Illumination	TiO_2 ST-NT, k (s^{-1})	r	TiO_2 ST-NT@Fe_3O_4NPs, k (s^{-1})	r
Blue light	8.1×10^{-5}	0.996	2.7×10^{-4}	0.982
Green light	2.1×10^{-5}	0.869	1.8×10^{-5}	0.983
White light	6.2×10^{-4}	0.980	—	—

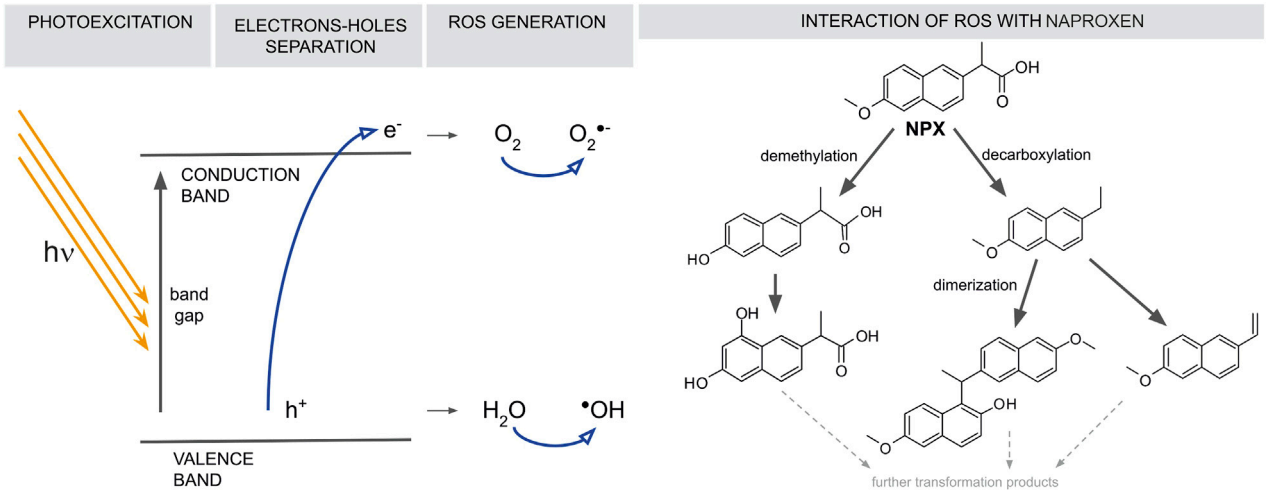

FIGURE 5
Semiconducting material photoexcitation mechanism. Upon an absorption of light of energy higher than the material's band gap, an electron (e^-) is excited to the conduction band, leaving a hole (h^+). These species further react with either oxygen or water, leading to the generation of reactive oxygen species (ROS). ROS attacks organic molecules–here, NPX (Kanakaraju et al., 2016a; Changanaqui et al., 2020; Jung et al., 2020).

promise for successful implementation into wastewater treatment procedures.

4 Conclusion

TiO_2 ST-NT and TiO_2 ST-NT@Fe_3O_4NPs powders annealed at 600°C were used as catalysts for the degradation of naproxen (NPX) using the blue, green, or white light, for the first time. The photocatalytic performance of TiO_2 ST-NT and TiO_2 ST-NT@Fe_3O_4NPs powders examined under the blue light showed a 60% and 92% reduction in NPX initial concentration within 3 h, respectively. This clearly indicates that the incorporation of Fe_3O_4 NPs enhanced the photocatalytic activity of TiO_2 ST-NT powders under the blue light. Under the green light, both TiO_2 ST-NT and TiO_2 ST-NT@$Fe_3O_4$4NPs powders only exhibited a 20% NPX degradation. Complete removal of NPX and one of its transformation products were observed in the experiment conducted using TiO_2 ST-NT powders and white light. Remarkably, 94% of NPX degraded within only 1 h. These findings demonstrate the immense potential of TiO_2 ST-NT powders for successful implementation in wastewater treatment.

Data availability statement

The original contributions presented in the study are included in the article/Supplementary Material, further inquiries can be directed to the corresponding author.

Author contributions

MS: Conceptualization, Writing–review and editing, Investigation, Methodology, Validation, Writing–original draft. JoM: Conceptualization, Investigation, Methodology, Writing–original draft, Writing–review and editing. IS: Investigation, Writing–review and editing. PC: Investigation, Writing–review and editing. JR-P: Investigation, Writing–review and editing, Visualization. HS: Writing–review and editing, Methodology, Supervision. BS: Methodology, Supervision, Writing–review and editing, Funding acquisition. JaM: Funding acquisition, Supervision, Writing–review and editing, Conceptualization, Project administration, Resources.

Funding

The author(s) declare financial support was received for the research, authorship, and/or publication of this article. The authors were supported by the Ministry of Education, Youth and Sports of the Czech Republic (projects LM2023037 and LM2023051).

Acknowledgments

The authors acknowledge the Ministry of Education, Youth and Sports of the Czech Republic for supporting CEMNAT (nr. LM2023037) and Czech Nano Lab (nr. LM2023051) infrastructures. The authors thank MSc Aleksandra Wójta for her help in conducting the photocatalytic experiments and Dr. Dariusz T. Mlynarczyk for his support and fruitful discussions.

Conflict of interest

The authors declare that the research was conducted in the absence of any commercial or financial relationships that could be construed as a potential conflict of interest.

The author(s) declared that they were an editorial board member of Frontiers, at the time of submission. This had no impact on the peer review process and the final decision.

Publisher's note

All claims expressed in this article are solely those of the authors and do not necessarily represent those of their affiliated organizations, or those of the publisher, the editors and the reviewers. Any product that may be evaluated in this article, or claim that may be made by its manufacturer, is not guaranteed or endorsed by the publisher.

Supplementary material

The Supplementary Material for this article can be found online at: https://www.frontiersin.org/articles/10.3389/fenvc.2024.1373320/full#supplementary-material

References

Abromaitis, V., Svaikauskaite, J., Sulciute, A., Sinkeviciute, D., Zmuidzinaviciene, N., Misevicius, S., et al. (2022). Ozone-enhanced TiO_2 nanotube arrays for the removal of COVID-19 aided antibiotic ciprofloxacin from water: process implications and toxicological evaluation. *J. Environ. Manage* 318, 115515. doi:10.1016/j.jenvman.2022.115515

Ai, Q., Yuan, Z., Huang, R., Yang, C., Jiang, G., Xiong, J., et al. (2019). One-pot co-precipitation synthesis of Fe_3O_4 nanoparticles embedded in 3D carbonaceous matrix as anode for lithium ion batteries. *J. Mat. Sci.* 54, 4212–4224. doi:10.1007/s10853-018-3141-3

Akpan, U. G., and Hameed, B. H. (2010). The advancements in sol–gel method of doped-TiO_2 photocatalysts. *Appl. Catal. A Gen.* 375, 1–11. doi:10.1016/j.apcata.2009.12.023

Albu, S. P., Ghicov, A., Macak, J. M., Hahn, R., and Schmuki, P. (2007). Self-organized, free-standing TiO_2 nanotube membrane for flow-through photocatalytic applications. *Nano Lett.* 7, 1286–1289. doi:10.1021/nl070264k

Amini, Z., Givianrad, M. H., Husain, S. W., Azar, P. A., and Saber-Tehrani, M. (2020). Cu-S codoping TiO_2/SiO_2 and TiO_2/SiO_2/Fe_3O_4 core-shell nanocomposites as a novel purple LED illumination active photocatalyst for degradation of diclofenac: the effect of different scavenger agents and optimization. *Chem. Eng. Commun.* 207, 1536–1553. doi:10.1080/00986445.2019.1660652

Anjali, R., and Shanthakumar, S. (2019). Insights on the current status of occurrence and removal of antibiotics in wastewater by advanced oxidation processes. *J. Environ. Manage* 246, 51–62. doi:10.1016/j.jenvman.2019.05.090

Arany, E., Szabó, R. K., Apáti, L., Alapi, T., Ilisz, I., Mazellier, P., et al. (2013). Degradation of naproxen by UV, VUV photolysis and their combination. *J. Hazard Mater* 262, 151–157. doi:10.1016/j.jhazmat.2013.08.003

Beketova, D., Motola, M., Sopha, H., Michalicka, J., Cicmancova, V., Dvorak, F., et al. (2020). One-step decoration of TiO_2 nanotubes with Fe_3O_4 nanoparticles: synthesis and photocatalytic and magnetic properties. *ACS Appl. Nano Mat.* 3, 1553–1563. doi:10.1021/acsanm.9b02337

Bi, J., Huang, X., Wang, J., Wang, T., Wu, H., Yang, J., et al. (2019). Oil-phase cyclic magnetic adsorption to synthesize Fe_3O_4@ C@ TiO_2-nanotube composites for simultaneous removal of Pb (II) and Rhodamine B. *Chem. Eng. J.* 366, 50–61. doi:10.1016/j.cej.2019.02.017

Cazzaniga, N., Varga, Z., Nicol, E., and Bouchonnet, S. (2020). UV-visible photodegradation of naproxen in water–Structural elucidation of photoproducts and potential toxicity. *Eur. J. Mass Spectrom.* 26, 400–408. doi:10.1177/1469066720973412

Changanaqui, K., Alarcon, H., Brillas, E., and Sires, I. (2020). Blue LED light-driven photoelectrocatalytic removal of naproxen from water: kinetics and primary by-products. *J. Electroanal. Chem.* 867, 114192. doi:10.1016/j.jelechem.2020.114192

Choi, H., Stathatos, E., and Dionysiou, D. D. (2007). Photocatalytic TiO_2 films and membranes for the development of efficient wastewater treatment and reuse systems. *Desalination* 202, 199–206. doi:10.1016/j.desal.2005.12.055

Coleman, H. M., Vimonses, V., Leslie, G., and Amal, R. (2007). Removal of contaminants of concern in water using advanced oxidation techniques. *Water Sci. Technol.* 55, 301–306. doi:10.2166/wst.2007.421

Collins-Martinez, V., López Ortiz, A., and Aguilar Elguézabal, A. (2007). Influence of the anatase/rutile ratio on the TiO_2 photocatalytic activity for the photodegradation of light hydrocarbons. *Int. J. Chem. React. Eng.* 5, 1–11. doi:10.2202/1542-6580.1613

Cory, W. C., Welch, A. M., Ramirez, J. N., and Rein, L. C. (2019). Naproxen and its phototransformation products: persistence and ecotoxicity to toad tadpoles (Anaxyrus terrestris), individually and in mixtures. *Environ. Toxicol. Chem.* 38, 2008–2019. doi:10.1002/etc.4514

Das, S., Sopha, H., Krbal, M., Zazpe, R., Podzemna, V., Prikryl, J., et al. (2017). Electrochemical infilling of $CuInSe_2$ within TiO_2 nanotube layers and subsequent photoelectrochemical studies. *ChemElectroChem* 4, 495–499. doi:10.1002/celc.201600763

DellaGreca, M., Brigante, M., Isidori, M., Nardelli, A., Previtera, L., Rubino, M., et al. (2003). Phototransformation and ecotoxicity of the drug Naproxen-Na. *Environ. Chem. Lett.* 1, 237–241. doi:10.1007/s10311-003-0045-4

Doh, S. J., Kim, C., Lee, S. G., Lee, S. J., and Kim, H. (2008). Development of photocatalytic TiO_2 nanofibers by electrospinning and its application to degradation of dye pollutants. *J. Hazard Mat.* 154, 118–127. doi:10.1016/j.jhazmat.2007.09.118

Eskandarian, M. R., Choi, H., Fazli, M., and Rasoulifard, M. H. (2016). Effect of UV-LED wavelengths on direct photolytic and TiO_2 photocatalytic degradation of emerging contaminants in water. *Chem. Eng. J.* 300, 414–422. doi:10.1016/j.cej.2016.05.049

Eslami, A., Amini, M. M., Asadi, A., Safari, A. A., and Daglioglu, N. (2020). Photocatalytic degradation of ibuprofen and naproxen in water over NS-TiO_2 coating on polycarbonate: process modeling and intermediates identification. *Inorg. Chem. Commun.* 115, 107888. doi:10.1016/j.inoche.2020.107888

Fan, G., Zhan, J., Luo, J., Zhang, J., Chen, Z., and You, Y. (2019). Photocatalytic degradation of naproxen by a H_2O_2-modified titanate nanomaterial under visible light irradiation. *Catal. Sci. Technol.* 9, 4614–4628. doi:10.1039/C9CY00965E

García-Valverde, M. T., Lucena, R., Galán-Cano, F., Cárdenas, S., and Valcárcel, M. (2014). Carbon coated titanium dioxide nanotubes: synthesis, characterization and potential application as sorbents in dispersive micro solid phase extraction. *J. Chromatogr. A* 1343, 26–32. doi:10.1016/j.chroma.2014.03.062

Ge, M., Hu, Z., Wei, J., He, Q., and He, Z. (2021). Recent advances in persulfate-assisted TiO_2-based photocatalysis for wastewater treatment: performances, mechanism and perspectives. *J. Alloys Compd.* 888, 161625. doi:10.1016/j.jallcom.2021.161625

Hao, X., Tian, J., Zhao, Y., Jing, T., Zheng, Y., and Lu, Z. (2023). Photocatalytic degradation of tetracycline over Ce-doped TiO_2@ SiO_2@ Fe_3O_4 magnetic material. *New J. Chem.* 47, 5939–5945. doi:10.1039/D3NJ00110E

Hashimoto, K., Irie, H., and Fujishima, A. (2005). TiO_2 photocatalysis: a historical overview and future prospects. *Jpn. J. Appl. Phys.* 44, 8269. doi:10.1143/JJAP.44.8269

Hoyos, L. J., Rivera, D. F., Gualdrón-Reyes, A. F., Ospina, R., Rodríguez-Pereira, J., Ropero-Vega, J. L., et al. (2017). Influence of immersion cycles during n–β–Bi_2O_3 sensitization on the photoelectrochemical behaviour of N–F–codoped TiO_2 nanotubes. *Appl. Surf. Sci.* 423, 917–926. doi:10.1016/j.apsusc.2017.06.209

Im, J.-K., Yoon, J., Her, N., Han, J., Zoh, K.-D., and Yoon, Y. (2015a). Sonocatalytic-TiO_2 nanotube, Fenton, and CCl_4 reactions for enhanced oxidation, and their applications to acetaminophen and naproxen degradation. *Sep. Purif. Technol.* 141, 1–9. doi:10.1016/j.seppur.2014.11.021

Isidori, M., Lavorgna, M., Nardelli, A., Parrella, A., Previtera, L., and Rubino, M. (2005). Ecotoxicity of naproxen and its phototransformation products. *Sci. total Environ.* 348, 93–101. doi:10.1016/j.scitotenv.2004.12.068

Jallouli, N., Elghniji, K., Hentati, O., Ribeiro, A. R., Silva, A. M. T., and Ksibi, M. (2016a). UV and solar photo-degradation of naproxen: TiO_2 catalyst effect, reaction kinetics, products identification and toxicity assessment. *J. Hazard Mat.* 304, 329–336. doi:10.1016/j.jhazmat.2015.10.045

Jung, S.-C., Bang, H.-J., Lee, H., Kim, H., Ha, H.-H., Yu, Y. H., et al. (2020). Degradation behaviors of naproxen by a hybrid TiO_2 photocatalyst system with process components. *Sci. Total Environ.* 708, 135216. doi:10.1016/j.scitotenv.2019.135216

Kanakaraju, D., Motti, C. A., Glass, B. D., and Oelgemöller, M. (2015). TiO_2 photocatalysis of naproxen: effect of the water matrix, anions and diclofenac on degradation rates. *Chemosphere* 139, 579–588. doi:10.1016/j.chemosphere.2015.07.070

Kanakaraju, D., Motti, C. A., Glass, B. D., and Oelgemöller, M. (2016a). Solar photolysis versus TiO_2-mediated solar photocatalysis: a kinetic study of the degradation of naproxen and diclofenac in various water matrices. *Environ. Sci. Pollut. Res.* 23, 17437–17448. doi:10.1007/s11356-016-6906-8

Kasuga, T., Hiramatsu, M., Hoson, A., Sekino, T., and Niihara, K. (1999). Titania nanotubes prepared by chemical processing. *Adv. Mater.* 11, 1307–1311. doi:10.1002/(SICI)1521-4095(199910)11:15<1307::AID-ADMA1307>3.0.CO;2-H

Kowalkińska, M., Sikora, K., Łapiński, M., Karczewski, J., and Zielińska-Jurek, A. (2023). Non-toxic fluorine-doped TiO_2 nanocrystals from $TiOF_2$ for facet-dependent naproxen degradation. *Catal. Today* 413, 113959. doi:10.1016/j.cattod.2022.11.020

Krakowiak, R., Frankowski, R., Mylkie, K., Mlynarczyk, D. T., Ziegler-Borowska, M., Zgoła-Grześkowiak, A., et al. (2022). TiO_2–Fe_3O_4 composite systems—preparation, physicochemical characterization, and an attempt to explain the limitations that arise in catalytic applications. *Appl. Sci.* 12, 8826. doi:10.3390/app12178826

Legrini, O., Oliveros, E., and Braun, A. M. (1993). Photochemical processes for water treatment. *Chem. Rev.* 93, 671–698. doi:10.1021/cr00018a003

Li, C.-J., Xu, G.-R., Zhang, B., and Gong, J. R. (2012). High selectivity in visible-light-driven partial photocatalytic oxidation of benzyl alcohol into benzaldehyde over single-crystalline rutile TiO_2 nanorods. *Appl. Catal. B* 115, 201–208. doi:10.1016/j.apcatb.2011.12.003

Li, X. Z., and Li, F. B. (2001). Study of Au/Au^{3+}-TiO^2 photocatalysts toward visible photooxidation for water and wastewater treatment. *Environ. Sci. Technol.* 35, 2381–2387. doi:10.1021/es001752w

Li, Z.-J., Huang, Z.-W., Guo, W.-L., Wang, L., Zheng, L.-R., Chai, Z.-F., et al. (2017). Enhanced photocatalytic removal of uranium (VI) from aqueous solution by magnetic TiO_2/Fe_3O_4 and its graphene composite. *Environ. Sci. Technol.* 51, 5666–5674. doi:10.1021/acs.est.6b05313

Liu, Y., Wan, J.-F., Liu, C.-T., and Li, Y.-B. (2016). Fabrication of magnetic Fe_3O_4/C/TiO_2 composites with nanotube structure and enhanced photocatalytic activity. *Mater. Sci. Technol.* 32, 786–793. doi:10.1179/1743284715Y.0000000089

Macak, J. M., Hildebrand, H., Marten-Jahns, U., and Schmuki, P. (2008). Mechanistic aspects and growth of large diameter self-organized TiO_2 nanotubes. *J. Electroanal. Chem.* 621, 254–266. doi:10.1016/j.jelechem.2008.01.005

Macak, J. M., Zlamal, M., Krysa, J., and Schmuki, P. (2007). Self-organized TiO_2 nanotube layers as highly efficient photocatalysts. *small* 3, 300–304. doi:10.1002/smll.200600426

Maculewicz, J., Kowalska, D., Świacka, K., Tański, M., Stepnowski, P., Białk-Bielińska, A., et al. (2022). Transformation products of pharmaceuticals in the environment: their fate,(eco) toxicity and bioaccumulation potential. *Sci. total Environ.* 802, 149916. doi:10.1016/j.scitotenv.2021.149916

Margot, J., Rossi, L., Barry, D. A., and Holliger, C. (2015). A review of the fate of micropollutants in wastewater treatment plants. *Wiley Interdiscip. Rev. Water* 2, 457–487. doi:10.1002/wat2.1090

Memmert, U., Peither, A., Burri, R., Weber, K., Schmidt, T., Sumpter, J. P., et al. (2013). Diclofenac: new data on chronic toxicity and bioconcentration in fish. *Environ. Toxicol. Chem.* 32, 442–452. doi:10.1002/etc.2085

Méndez-Arriaga, F., Esplugas, S., and Giménez, J. (2008a). Photocatalytic degradation of non-steroidal anti-inflammatory drugs with TiO_2 and simulated solar irradiation. *Water Res.* 42, 585–594. doi:10.1016/j.watres.2007.08.002

Méndez-Arriaga, F., Gimenez, J., and Esplugas, S. (2008b). Photolysis and TiO_2 photocatalytic treatment of naproxen: degradation, mineralization, intermediates and toxicity. *J. Adv. Oxid. Technol.* 11, 435–444. doi:10.1515/jaots-2008-0302

Miklos, D. B., Remy, C., Jekel, M., Linden, K. G., Drewes, J. E., and Hübner, U. (2018). Evaluation of advanced oxidation processes for water and wastewater treatment–A critical review. *Water Res.* 139, 118–131. doi:10.1016/j.watres.2018.03.042

Mills, A., Davies, R. H., and Worsley, D. (1993). Water purification by semiconductor photocatalysis. *Chem. Soc. Rev.* 22, 417–425. doi:10.1039/CS9932200417

Mills, A., and Le Hunte, S. (1997). An overview of semiconductor photocatalysis. *J. Photochem. Photobiol. A Chem.* 108, 1–35. doi:10.1016/S1010-6030(97)00118-4

Molinari, R., Pirillo, F., Loddo, V., and Palmisano, L. (2006). Heterogeneous photocatalytic degradation of pharmaceuticals in water by using polycrystalline TiO_2 and a nanofiltration membrane reactor. *Catal. Today* 118, 205–213. doi:10.1016/j.cattod.2005.11.091

Motola, M., Sopha, H., Krbal, M., Hromádko, L., Zmrhalová, Z. O., Plesch, G., et al. (2018). Comparison of photoelectrochemical performance of anodic single- and double-walled TiO_2 nanotube layers. *Electrochem. Commun.* 97, 1–5. doi:10.1016/j.elecom.2018.09.015

Musial, J., Krakowiak, R., Frankowski, R., Spychala, M., Dlugaszewska, J., Dobosz, B., et al. (2022). Simple modification of titanium (IV) oxide for the preparation of a reusable photocatalyst. *Mater. Sci. Eng. B* 276, 115559. doi:10.1016/j.mseb.2021.115559

Musial, J., Mlynarczyk, D. T., and Stanisz, B. J. (2023). Photocatalytic degradation of sulfamethoxazole using TiO2-based materials–Perspectives for the development of a sustainable water treatment technology. *Sci. Total Environ.* 856, 159122. doi:10.1016/j.scitotenv.2022.159122

Ni, M., Leung, M. K. H., Leung, D. Y. C., and Sumathy, K. (2007). A review and recent developments in photocatalytic water-splitting using TiO_2 for hydrogen production. *Renew. Sustain. Energy Rev.* 11, 401–425. doi:10.1016/j.rser.2005.01.009

Olusegun, S. J., Souza, T. G. F., Souza, G. de O., Osial, M., Mohallem, N. D. S., Ciminelli, V. S. T., et al. (2023). Iron-based materials for the adsorption and photocatalytic degradation of pharmaceutical drugs: a comprehensive review of the mechanism pathway. *J. Water Process Eng.* 51, 103457. doi:10.1016/j.jwpe.2022.103457

Pena-Velasco, G., Hinojosa-Reyes, L., Moran-Quintanilla, G. A., Hernandez-Ramirez, A., Villanueva-Rodriguez, M., and Guzman-Mar, J. L. (2021). Synthesis of heterostructured catalyst coupling MOF derived Fe_2O_3 with TiO_2 for enhanced photocatalytic activity in anti-inflammatory drugs mixture degradation. *Ceram. Int.* 47 (17), 24632–24640. doi:10.1016/j.ceramint.2021.05.185

Petrie, B., Barden, R., and Kasprzyk-Hordern, B. (2015). A review on emerging contaminants in wastewaters and the environment: current knowledge, understudied areas and recommendations for future monitoring. *Water Res.* 72, 3–27. doi:10.1016/j.watres.2014.08.053

Punjabi, P. B., Ameta, R., Chohadia, A. K., and Jain, A. (2018). *Fenton and photo-fenton processes*. Rajasthan, India: Udaipur.

Qian, X., Xu, L., Zhu, Y., Yu, H., and Niu, J. (2021). Removal of aqueous triclosan using TiO_2 nanotube arrays reactive membrane by sequential adsorption and electrochemical degradation. *Chem. Eng. J.* 420, 127615. doi:10.1016/j.cej.2020.127615

Rouxhet, P. G., and Genet, M. J. (2011). XPS analysis of bio-organic systems. *Surf. Interface Analysis* 43, 1453–1470. doi:10.1002/sia.3831

Sepúlveda, M., Saldan, I., Mahnaz, A., Cicmancova, V., Michalicka, J., Hromadko, L., et al. (2023). Magnetically guidable single TiO_2 nanotube photocatalyst: structure and photocatalytic properties. *Ceram. Int.* 49, 6764–6771. doi:10.1016/j.ceramint.2022.10.197

Sheydaei, M., Haseli, A., Ayoubi-Feiz, B., and Vatanpour, V. (2022). MoS_2/N-TiO_2/Ti mesh plate for visible-light photocatalytic ozonation of naproxen and industrial wastewater: comparative studies and artificial neural network modeling. *Environ. Sci. Pollut. Res.* 29, 22454–22468. doi:10.1007/s11356-021-17285-w

Simon, J. P., and Evan Prince, S. (2017). Natural remedies for non-steroidal anti-inflammatory drug-induced toxicity. *J. Appl. Toxicol.* 37, 71–83. doi:10.1002/jat.3391

Solís-Casados, D. A., Escobar-Alarcón, L., Gómez-Oliván, L. M., Haro-Poniatowski, E., and Klimova, T. (2017). Photodegradation of pharmaceutical drugs using Sn-modified TiO_2 powders under visible light irradiation. *Fuel* 198, 3–10. doi:10.1016/j.fuel.2017.01.059

Sopha, H., Bacova, J., Baishya, K., Sepúlveda, M., Rodriguez-Pereira, J., Capek, J., et al. (2023). White and black anodic TiO_2 nanotubes: comparison of biological effects in A549 and SH-SY5Y cells. *Surf. Coat. Technol.* 462, 129504. doi:10.1016/j.surfcoat.2023.129504

Sopha, H., Mirza, I., Turčičova, H., Pavlinak, D., Michalicka, J., Krbal, M., et al. (2020). Laser-induced crystallization of anodic TiO_2 nanotube layers. *RSC Adv.* 10, 22137–22145. doi:10.1039/D0RA02929G

Stasinakis, A. S. (2008). Use of selected advanced oxidation processes (AOPs) for wastewater treatment–a mini review. *Glob. NEST J.* 10, 376–385. doi:10.30955/gnj.000598

Stovitz, S. D., and Johnson, R. J. (2003). NSAIDs and musculoskeletal treatment: what is the clinical evidence? *Phys. Sportsmed.* 31, 35–52. doi:10.3810/psm.2003.01.160

Tanaka, K., Capule, M. F. V., and Hisanaga, T. (1991). Effect of crystallinity of TiO_2 on its photocatalytic action. *Chem. Phys. Lett.* 187, 73–76. doi:10.1016/0009-2614(91)90486-S

Tang, X. Q., Zhang, Y. D., Jiang, Z. W., Wang, D. M., Huang, C. Z., and Li, Y. F. (2018). Fe_3O_4 and metal–organic framework MIL-101 (Fe) composites catalyze luminol chemiluminescence for sensitively sensing hydrogen peroxide and glucose. *Talanta* 179, 43–50. doi:10.1016/j.talanta.2017.10.049

Todd, P. A., and Clissold, S. P. (1990). Naproxen A reappraisal of its pharmacology, and therapeutic use in rheumatic diseases and pain states. *Drugs* 40, 91–137. doi:10.2165/00003495-199040010-00006

Uheida, A., Mohamed, A., Belaqziz, M., and Nasser, W. S. (2019). Photocatalytic degradation of Ibuprofen, Naproxen, and Cetirizine using PAN-MWCNT nanofibers crosslinked TiO_2-NH_2 nanoparticles under visible light irradiation. *Sep. Purif. Technol.* 212, 110–118. doi:10.1016/j.seppur.2018.11.030

Wu, C.-Y., Tu, K.-J., Deng, J.-P., Lo, Y.-S., and Wu, C.-H. (2017). Markedly enhanced surface hydroxyl groups of TiO_2 nanoparticles with superior water-dispersibility for photocatalysis. *Materials* 10, 566. doi:10.3390/ma10050566

Ye, Y., Feng, Y., Bruning, H., Yntema, D., and Rijnaarts, H. H. M. (2018). Photocatalytic degradation of metoprolol by TiO_2 nanotube arrays and UV-LED: effects of catalyst properties, operational parameters, commonly present water constituents, and photo-induced reactive species. *Appl. Catal. B* 220, 171–181. doi:10.1016/j.apcatb.2017.08.040

Yilmaz, E., Salem, S., Sarp, G., Aydin, S., Sahin, K., Korkmaz, I., et al. (2020). TiO_2 nanoparticles and C-Nanofibers modified magnetic Fe_3O_4 nanospheres (TiO_2@ Fe_3O_4@ C–NF): a multifunctional hybrid material for magnetic solid-phase extraction of ibuprofen and photocatalytic degradation of drug molecules and azo dye. *Talanta* 213, 120813. doi:10.1016/j.talanta.2020.120813

Yu, H.-W., Park, M., Wu, S., Lopez, I. J., Ji, W., Scheideler, J., et al. (2019). Strategies for selecting indicator compounds to assess attenuation of emerging contaminants during UV advanced oxidation processes. *Water Res.* 166, 115030. doi:10.1016/j.watres.2019.115030

Zaveri, B. K., De Souza, N. G., Parenky, A. C., and Choi, H. (2018). LED-Based ultraviolet oxidation of pharmaceuticals: effects of wavelength and intensity, pH, and TiO_2 loading. *Water Environ. Res.* 90, 790–799. doi:10.2175/106143017X15131012187926

Zhou, W., Pan, K., Qu, Y., Sun, F., Tian, C., Ren, Z., et al. (2010). Photodegradation of organic contamination in wastewaters by bonding TiO2/single-walled carbon nanotube composites with enhanced photocatalytic activity. *Chemosphere* 81, 555–561. doi:10.1016/j.chemosphere.2010.08.059